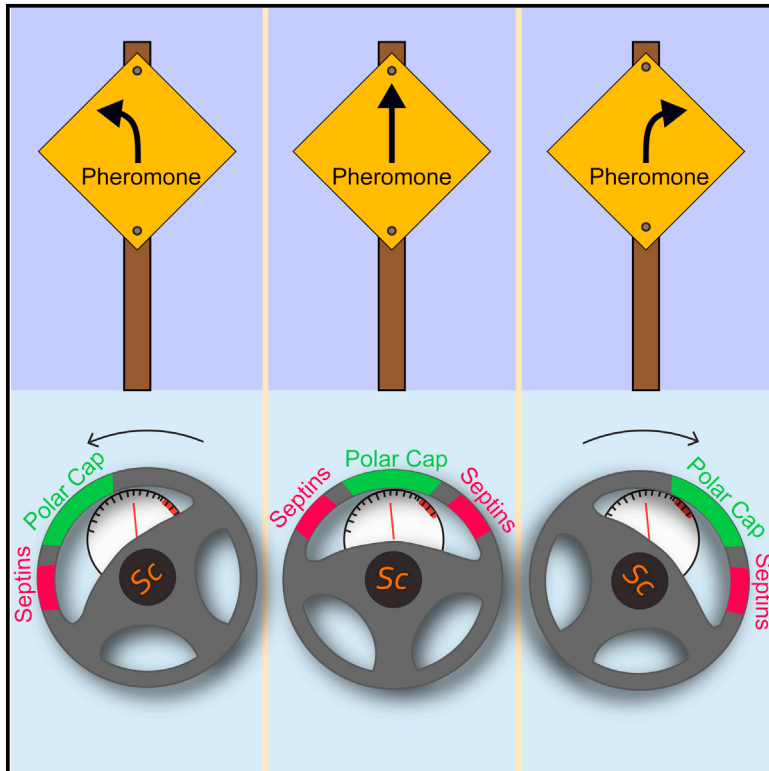


Current Biology

RGS Proteins and Septins Cooperate to Promote Chemotropism by Regulating Polar Cap Mobility

Graphical Abstract



Authors

Joshua B. Kelley, Gauri Dixit, ..., Timothy C. Elston, Henrik G. Dohlman

Correspondence

timothy_elston@med.unc.edu (T.C.E.), henrik_dohlman@med.unc.edu (H.G.D.)

In Brief

Yeast use GPCRs (G protein-coupled receptors) to detect pheromone from potential mating partners, and GPCR signaling is attenuated by RGS (regulator of G protein signaling) proteins. Less is known about how cells track a gradient stimulus. Kelley et al. show that RGS proteins promote tracking by regulating the organization of septins, which direct polar cap mobility.

Highlights

- RGS proteins regulate the organization of septin structures
- Septins bias polar cap movement during chemotropic growth
- RGS and septins cooperate to promote gradient tracking

RGS Proteins and Septins Cooperate to Promote Chemotropism by Regulating Polar Cap Mobility

Joshua B. Kelley,^{1,2} Gauri Dixit,¹ Joshua B. Sheetz,¹ Sai Phanindra Venkatapurapu,^{2,3} Timothy C. Elston,^{2,*} and Henrik G. Dohlman^{1,2,*}

¹Department of Biochemistry and Biophysics, University of North Carolina at Chapel Hill, 120 Mason Farm Road, 3046 Genetic Medicine Building, Campus Box 7260, Chapel Hill, NC 27599, USA

²Department of Pharmacology, University of North Carolina at Chapel Hill, 120 Mason Farm Road, 4009 Genetic Medicine Building, Campus Box 7365, Chapel Hill, NC 27599, USA

³Curriculum in Bioinformatics and Computational Biology, University of North Carolina at Chapel Hill, 120 Mason Farm Road, 4092 Genetic Medicine Building, Campus Box 7365, Chapel Hill, NC 27599, USA

Summary

Background: Septins are well known to form a boundary between mother and daughter cells in mitosis, but their role in other morphogenic states is poorly understood.

Results: Using microfluidics and live-cell microscopy, coupled with new computational methods for image analysis, we investigated septin function during pheromone-dependent chemotropic growth in yeast. We show that septins colocalize with the regulator of G protein signaling (RGS) Sst2, a GTPase-activating protein that dampens pheromone receptor signaling. We show further that the septin structure surrounds the polar cap, ensuring that cell growth is directed toward the source of pheromone. When RGS activity is abrogated, septins are partially disorganized. Under these circumstances, the polar cap travels toward septin structures and away from sites of exocytosis, resulting in a loss of gradient tracking.

Conclusions: Septin organization is dependent on RGS protein activity. When assembled correctly, septins promote turning of the polar cap and proper tracking of a pheromone gradient.

Introduction

To respond to spatial cues in their environment, cells must be capable of detecting and transforming those signals into an appropriate response. For example, neutrophils follow a gradient of secreted factors to find and destroy invading pathogens [1]. Similarly, the yeast *Saccharomyces cerevisiae* can expand toward a gradient of pheromone to find a mating partner [2, 3]. In this instance of yeast chemotropic growth, detection of the pheromone gradient is accomplished by a G protein-coupled receptor. The receptor activates a large G protein composed of an α subunit, Gpa1, and a $G\beta\gamma$ dimer of Ste4 and Ste18 [4]. Upon activation, Gpa1-GTP dissociates from the $G\beta\gamma$ dimer [5]. Free $G\beta\gamma$ then recruits scaffolds and kinases to initiate two effector pathways, one leading to activation of a mitogen-activated protein kinase and to transcriptional induction, and the second leading to activation of the

small G protein Cdc42 [5]. It is this second pathway that ensures proper expansion toward a pheromone gradient [2, 6]. In particular, $G\beta\gamma$ recruitment of the guanine nucleotide exchange factor Cdc24 ensures that activation of Cdc42 is spatially coupled to sites of receptor activation [7, 8]. Cdc42-GTP promotes actin polymerization and exocytosis, thereby defining the polarity of the cell [9]. Cdc42 and the machinery that drives its spatial distribution are collectively known as the polar cap [10].

The pheromone-induced morphogenesis pathway shares many components with the mitosis/budding machinery. However, whereas bud site formation occurs in response to an internal, static cue [11], chemotropic growth is dynamic so as to adapt to changing external signals [2, 12]. Such dynamic behavior is accomplished by pheromone signaling factors upstream of Cdc42 in the pathway. Aside from the pheromone receptor and G protein there are three proteins known to be required for gradient tracking: Fus3, Far1, and Sst2 [3, 13, 14]. Far1 is necessary for gradient tracking because it couples Cdc24 to free $G\beta\gamma$, which results in the production of Cdc42-GTP proximal to sites of pheromone binding [7, 15]. Without this cue the Cdc42 polarity machinery is spatially uncoupled from receptor activation, and the cells expand in a random direction [15, 16]. Fus3 is required to phosphorylate Far1, promoting release of Far1 from the nucleus and delivery to $G\beta\gamma$ [7, 13, 14, 16, 17]. The role of Sst2 is, by comparison, poorly understood. Sst2 is the founding member of the regulator of G protein signaling (RGS) family [18]. It binds to the pheromone receptor and also functions as a GTPase-activating protein (GAP) for Gpa1 [19, 20]. Both functions contribute equally to desensitization of the pathway [21]. However, it is the GAP activity alone that is required for proper gradient tracking [21].

In this study, we demonstrate that Sst2 promotes polarized cell expansion, and does so by organizing the localization of cytoskeletal scaffolding proteins known as septins [22, 23]. We thought to examine septins because of their well-characterized role during mitosis. Septins form a double-ring structure at the mother-daughter bud neck, serving as a diffusional barrier between the two cells [24] and constraining the movement of the polar cap [25, 26]. Likewise, septin bundles form at the base of the mating projection, or “shmoo” tip [27, 28]. In this case, septins are organized parallel to the axis of the shmoo and have no known barrier function [28]. Here we show that Sst2 GAP activity is required to maintain separation of the polar cap and septins. In the absence of GAP activity, septins distribute asymmetrically and the polar cap follows. Thus, Sst2 acts to limit movement of the polar cap and prevent aberrant turning from the pheromone gradient. Collectively, these findings reveal a new function for RGS proteins in membrane trafficking and cytoskeletal organization, as well as a new role for septins in gradient tracking behavior.

Results

Sst2 Promotes the Persistence of Polarized Growth

In preparation for mating, yeast cells stop dividing and instead form a pear-shaped structure, or shmoo, that is competent to fuse with cells of the opposite mating type. In addition to the

*Correspondence: timothy_elston@med.unc.edu (T.C.E.), henrik_dohlman@med.unc.edu (H.G.D.)



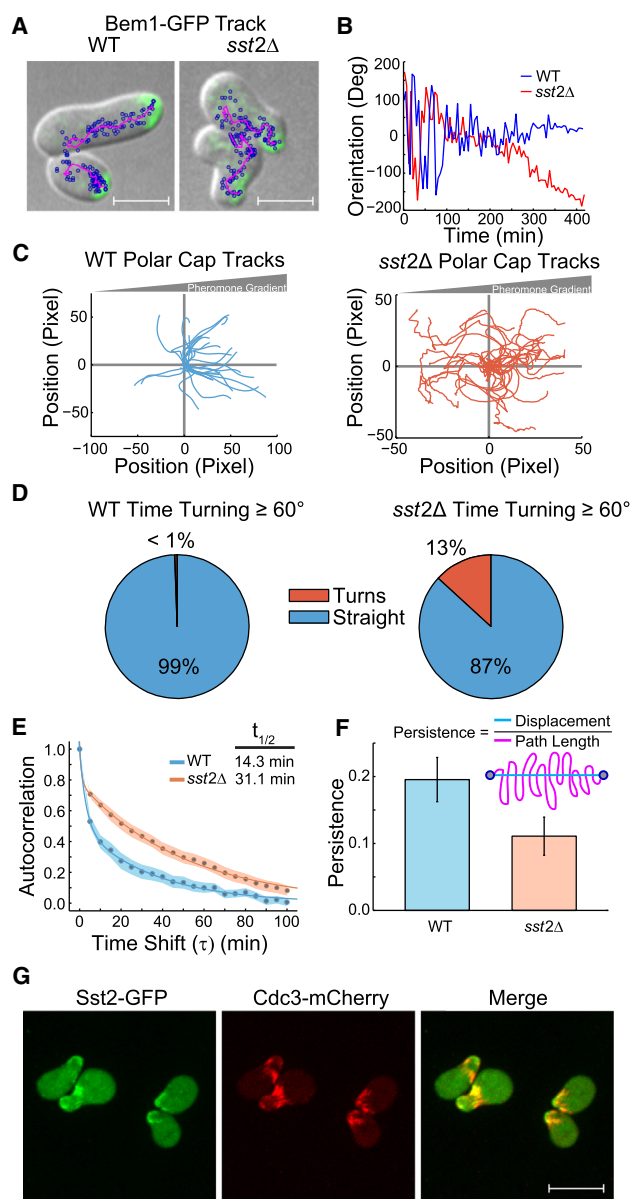


Figure 1. Sst2 Promotes Persistent Polarized Growth

(A) Live-cell imaging of the Cdc42-GTP scaffold Bem1-GFP (5 min time points for 12 hr) in a 0–150 nM α factor pheromone gradient. Shown are representative images for wild-type and *sst2Δ* cells at 7 hr (the gradient increases toward the right side). The centroid of the polar patch at each time point is overlaid on the images (blue circles). The magenta line is the time-averaged trajectory of the centroids. The scale bars represent 5 μ m.

(B) Single-cell analysis of the orientation of the polar patch (angle from the direction of the gradient) over time for wild-type and *sst2Δ* cells.

(C) Time-averaged tracks of the polar cap centroids for wild-type and *sst2Δ* cells. The gradient is high on the right side of the graphs.

(D) Frequency of large turns ($>60^\circ$) per time point (5 min) in wild-type and *sst2Δ* cells.

(E) Average autocorrelation for wild-type and *sst2Δ* cells ($n = 25$). The shaded areas indicate SEM.

(F) Persistence of the polar patch (final displacement/total distance traveled) for wild-type and *sst2Δ* cells ($n = 25$). Error bars indicate SEM. Data from (A)–(F) are derived from or representative of 25 individual cells from two (*sst2Δ*) or four (wild-type) independent experiments.

(G) Cells expressing Sst2-GFP and Cdc3-mCherry treated with pheromone for 2 hr and imaged on an agar pad. Images are representative of 19 fields of cells from two independent experiments. The scale bar represents 5 μ m. See also [Figures S1 and S4](#) and [Movies S1 and S2](#).

budding (no pheromone) and shmooing (high pheromone) morphologies, there exists a third morphogenic state, evident at intermediate pheromone concentrations, where cells have stopped dividing but continue to grow in the direction of a weak pheromone gradient [14]. We refer to this as “elongated” or “chemotropic” growth. During chemotropic growth, the polar cap wanders back and forth across the growing edge of the cell, and this behavior is required for gradient tracking [29]. Given that Sst2 is also required for cells to track a gradient [3, 21], we considered the role of Sst2 in controlling the movement of the polar cap. We began by comparing the distribution of the polar cap in wild-type cells and in mutant cells lacking Sst2 (*sst2Δ*). Experiments were performed in a custom-designed microfluidic device that produces a gradient across the cells [16, 21]. Using the microfluidic chamber, we exposed cells to a 0–150 nM gradient of pheromone and examined the localization of the Cdc42-GTP-binding protein Bem1 over time [30, 31]. We used the same gradient conditions throughout to ensure equal receptor occupancy. As shown in [Figure 1A](#), wild-type cells initially polarized to the site of cytokinesis but later redirected growth in the direction of the gradient ([Movie S1](#) available online). In contrast, the *sst2Δ* mutant cells turned frequently, and often abruptly, away from the gradient ([Figure 1A](#); [Movie S2](#)).

To quantify gradient tracking behaviors, we used four read-outs of polar cap function: angle of orientation, frequency of turning, memory, and persistence. The angle of orientation is defined as the angle between the polar cap (determined by the method shown in [Figure S1A](#)) and the direction of the gradient. Perfect alignment toward the gradient is defined as zero. As shown in [Figure 1B](#), wild-type cells became oriented within 100 min. However, in *sst2Δ* cells, the angle of orientation tended to move in a single direction across the periphery of the cell, and over an extended period of time ([Figure 1B](#)). This “spinning” behavior is evident from time-averaged polar cap tracks of individual cells shown in [Figure 1C](#). In cells lacking Sst2, the average path of the polar cap exhibited turns that were both sharper and more frequent than those seen in wild-type cells. To quantify the turning behavior, we next examined the frequency of turns greater than 60° . Whereas wild-type cells displayed large turns less than 1% of the time, cells lacking Sst2 displayed large turns 13% of the time ([Figure 1D](#)). A third measure of polar cap function is memory, or the time period for which the current angle of orientation is correlated with future angles of orientation (autocorrelation). By this measure, we found that the memory of *sst2Δ* cells was roughly twice that of wild-type ([Figure 1E](#)). That is, the polar cap sweeps uniformly in one direction for a longer period of time in *sst2Δ* cells. Finally, we measured persistence of growth, defined as the difference between the position of the polar cap at the beginning and end of a fixed time interval divided by the total length of the path traveled by the polar cap during that interval ([Figure 1F](#)). A persistence of 1 implies that the polar cap moved in a straight line during the time interval, and values less than 1 indicate polar cap wandering. As shown in [Figure 1F](#), cells lacking Sst2 displayed half the persistence of that shown by wild-type cells. Taken together, these data suggest that Sst2 constrains movement of the polar cap, thereby promoting directed expansion toward a stimulus.

Sst2 localization to the periphery of the cell is dependent upon interaction with the pheromone receptor Ste2 [20]. We have shown previously that Sst2 localization is highly dynamic, and after prolonged pheromone treatment the protein becomes concentrated at the base of the mating projection

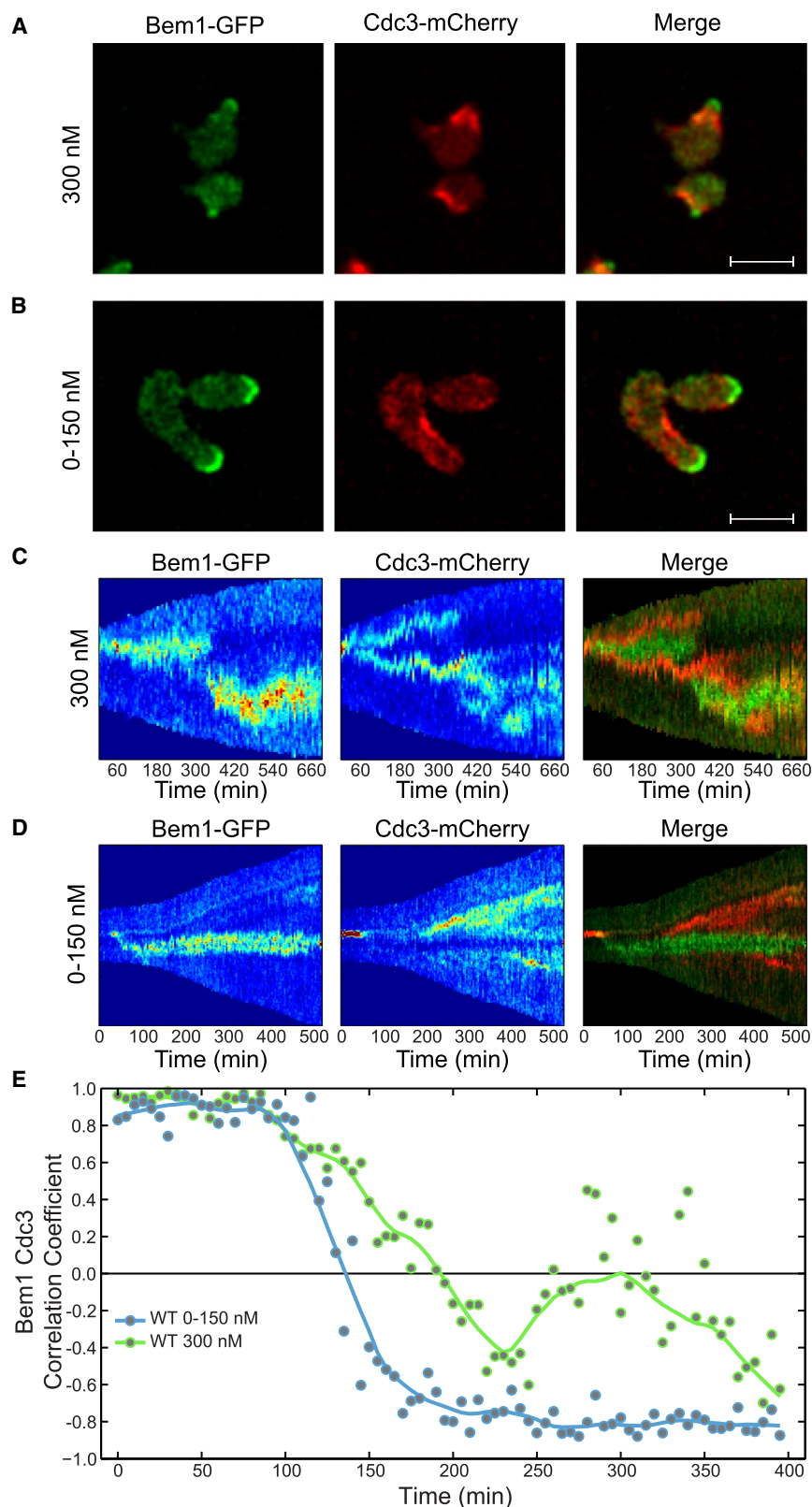


Figure 2. Septins Form Structures during Chemotropic Growth

(A and B) Wild-type cells expressing the polarity marker Bem1-GFP and the septin marker Cdc3-mCherry, imaged (A) at high pheromone (300 nM; 360 min pheromone treatment shown) to drive the formation of mating projections or (B) in a pheromone gradient (0–150 nM; 420 min pheromone treatment shown) to drive chemotropic growth in a microfluidic gradient chamber. The scale bars represent 5 μ m.

(C) Kymographs of Bem1-GFP and Cdc3-mCherry in high pheromone.

(D) Kymographs of Bem1-GFP and Cdc3-mCherry in a gradient of pheromone.

The merged kymographs are colored according to the fluorescent protein (green, Bem1; red, Cdc3).

(E) The average correlation between Bem1-GFP and Cdc3-mCherry over time. The late increase in correlation coefficient corresponds to the formation of a second mating projection. Images and kymographs are representative of, and the graphs are derived from, 25 cells from four independent experiments (0–150 nM) and 27 cells from two independent experiments (300 nM).

See also [Figure S2](#) and [Movies S3](#) and [S4](#).

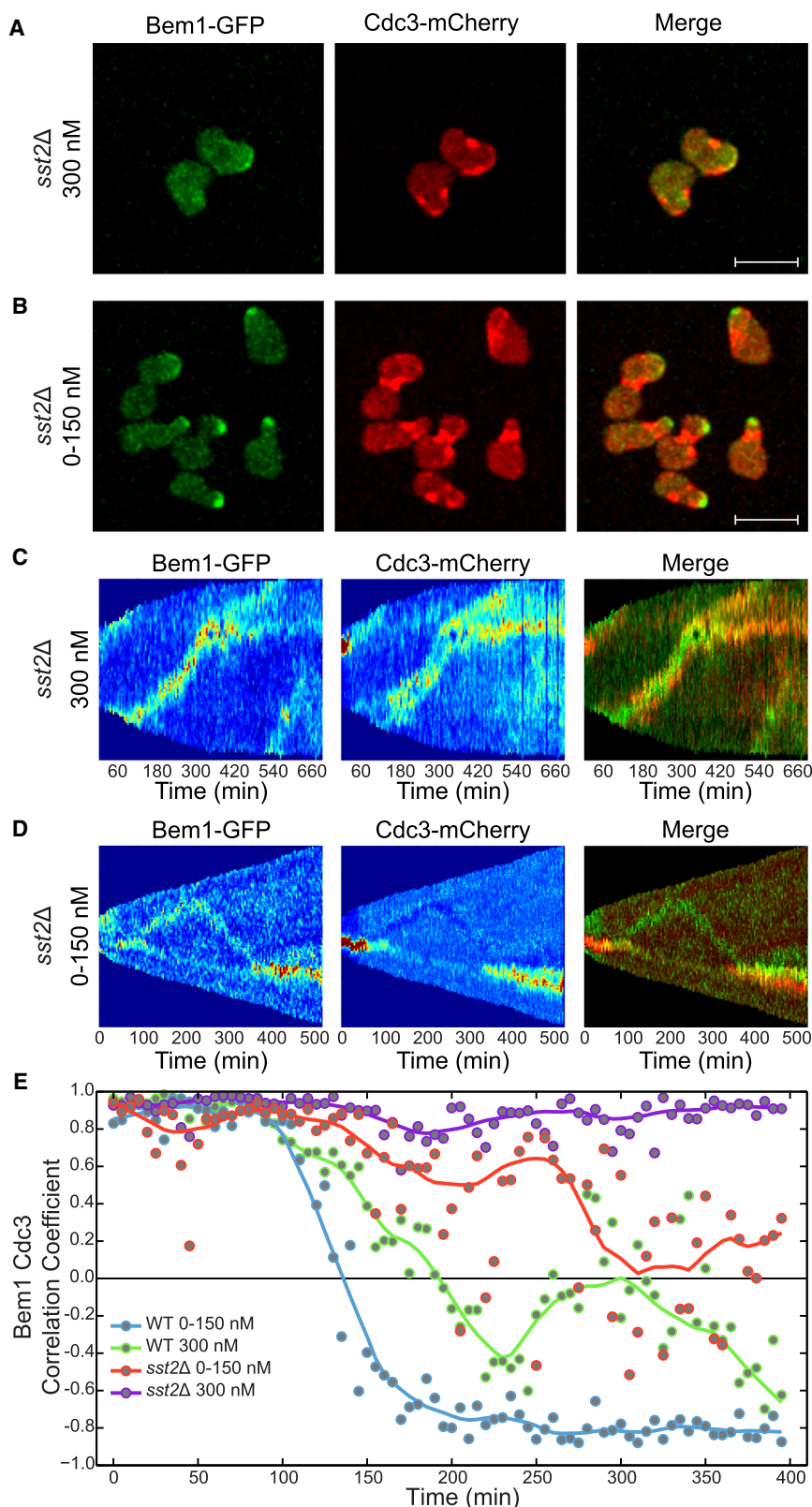
examine the functional relationship between these proteins, we began by monitoring Sst2-GFP localization in cells expressing the septin marker Cdc3-mCherry [32]. We observed overlapping localization of these proteins in shmooing ([Figure 1G](#)) and elongated cells ([Figures S1B](#) and [S1C](#)). By associating with the septin structure in this way, Sst2 may serve to restrict the movement of the polar cap past septins and drive it back toward the center of the shmoo tip.

Septin Structures Are Formed during Chemotropic Growth

Septins are known to form a bundled structure of fibers along the side of the shmoo at the base of the mating projection. This pattern of assembly is in contrast to the double-ring structure formed orthogonally to the mother-daughter axis in mitosis [23, 27, 28]. Although the septin structure formed at the base of the shmoo does not appear to be contiguous ([Figure 1G](#)) [28], and therefore is unlikely to form a physical diffusion barrier, scaffolding of the negative regulator Sst2 may serve to create a biochemical boundary around the polar cap. Accordingly, we next investigated whether septins form a defined structure during chemotropic growth, and whether

([Figure S2](#) in [21]). This subcellular distribution of Sst2 is reminiscent of septin localization [28]. The septin collar is well known to restrict polar cap movement during mitosis [25, 26], but little is known about the role of septin bundles in chemotropic growth or how their localization is regulated. To

that structure is required for gradient tracking. To that end, we monitored septins (using Cdc3-mCherry [32]) and the polar cap (using Bem1-GFP) over time. In high pheromone (300 nM uniform), septins formed structures at the base of the mating projection, as previously reported [27, 28] ([Figure 2A](#); [Movie S3](#)). In



a pheromone gradient (0–150 nM), septins formed discernible structures at the periphery of the elongated cells (Figure 2B; Movie S4). These structures appeared to be excluded from the sites of polarity, as defined by Bem1. To compare changes in the polar cap and septins over time, we plotted the

movement (Figure 1), we hypothesized that these cells might also be deficient in boundary function. To that end, we examined septin localization in the *sst2Δ* mutant strain (Figure 3). In this case, septins exhibited aberrant colocalization with the polar cap in high pheromone concentrations (Figures 3A and

Figure 3. Sst2 Is Required for Proper Septin Structure Formation

(A and B) *sst2Δ* cells expressing Bem1-GFP and Cdc3-mCherry imaged in a microfluidic gradient chamber (A) at high pheromone to drive the formation of mating projections or (B) in a pheromone gradient to drive chemotropic growth. The scale bars represent 5 μ m.

(C) Kymographs of *sst2Δ* cells in high pheromone. (D) Kymographs of *sst2Δ* cells in a gradient of pheromone.

(E) The average correlation between Bem1-GFP and Cdc3-mCherry over time comparing wild-type and *sst2Δ* cells. Images and kymographs are representative of, and the graphs are derived from, 25 cells from two independent experiments (0–150 nM) and 37 cells from two independent experiments (300 nM).

See also Movies S5 and S6.

distribution of Cdc3 and Bem1 as line scans taken around the cell boundary (kymographs) (Figures 2C and 2D). Note that the cells start in mitosis, so the strong initial septin staining represents the mitotic ring. These figures clearly demonstrate that, as cells elongate, the polar patch is constrained between regions of high Cdc3 concentration. To quantify these results, we calculated the correlation coefficient over time, between the polar cap and septins, from the average of many individual cells. As shown in Figure 2E, the correlation coefficient started high during mitosis, then decreased after ~ 100 min, and eventually became anticorrelated during chemotropic growth. Interestingly, this change coincides with a decrease in polar cap angle variation (Figure 1B), suggesting that septins help to stabilize the position of the polar cap. The anticorrelation was stronger in elongating (chemotropic) cells (Figure 2E, blue curve) than in shmooing cells (Figure 2E, green curve). This difference is likely due to the much larger surface area in elongating cells. Thus, it appears that septins form symmetric structures that surround and exclude the polar cap during chemotropic growth.

Sst2 Is Necessary for Proper Septin Organization

As shown above, septins and Sst2 co-localize to the boundary of the polar cap during both shmooing and elongated growth. Given that *sst2Δ* mutants fail to undergo persistent directional

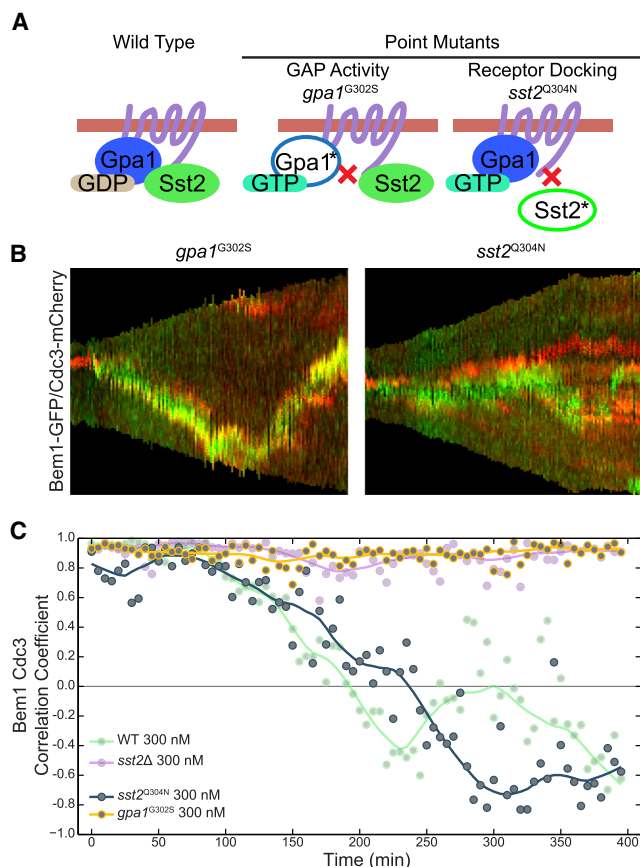


Figure 4. Sst2 GAP Activity Is Necessary for Proper Septin Structure Formation

(A) Schematic describing the point mutants used to uncouple Sst2 GAP activity (*gpa1^{G302S}*) and Sst2 receptor binding activity (*sst2^{Q304N}*). (B) Kymographs of Bem1-GFP and Cdc3-mCherry in the mutant strains at high pheromone. (C) The average correlation between Bem1 and Cdc3 over time. Kymographs are representative of, and the graphs are derived from, 36 cells from two independent experiments (*gpa1^{G302S}*) and 31 cells from two independent experiments (*sst2^{Q304N}*).

3C; [Movie S5](#)) as well as aberrant organization and occasional colocalization in a pheromone gradient ([Figures 3B and 3D](#); [Movie S6](#)). The prolonged loss of Cdc3 is distinct from the dispersal that typically occurs following mitosis ([Figure 2D](#)). In a high dose, the septin structure appeared to be mislocalized to the polar cap rather than forming a symmetric structure at the boundary. Under gradient conditions, cells alternated between elongation and turning, with random positioning of septin structures. The same aberrant behavior was seen after chitin staining, demonstrating that the septin misorganization is not an artifact of the fluorescently tagged Cdc3 ([Figure S2](#)). From these data, we conclude that Sst2 is necessary for proper septin localization and segregation from the polar cap during shmooing as well as during elongated growth.

GAP Activity Is Necessary for Proper Septin Structure Formation

Sst2 has two known binding partners. First, Sst2 binds to Gpa1 and accelerates GTPase activity [19]. Second, Sst2 binds to the C-terminal tail of the receptor Ste2 [20]. We have previously shown that these interactions contribute equally to attenuating

the response to pheromone but that GAP activity alone is needed for proper chemotropic growth [21]. Because deletion of Sst2 disrupts both functions, we used point mutants that selectively uncouple the interactions. The RGS mutant *sst2^{Q304N}* decreases Sst2 binding to the receptor while leaving RGS-G protein interactions intact [20]. The G protein mutant *gpa1^{G302S}* decreases Sst2 binding to the G protein α subunit ([Figure 4A](#)), abrogating RGS-stimulated GTPase activity but leaving both intrinsic GTPase activity and $G\beta\gamma$ binding unaltered [33]. As shown in [Figure 4B](#), cells bearing the receptor-uncoupled Sst2 mutant exhibited normal septin structures and separation from the polar cap. In contrast, cells expressing the unGAPable *gpa1^{G302S}* mutant exhibited abnormal septin structures and aberrant colocalization of the polar cap and septins ([Figure 4B](#)). The altered localization persisted throughout the experiment ([Figure 4C](#), yellow curve), as seen in the *sst2Δ* cells ([Figure 4C](#), purple curve). Because the *sst2^{Q304N}* and *gpa1^{G302S}* strains are equally sensitive to pheromone [21], the defect exhibited by *gpa1^{G302S}* is not due to altered signaling strength. Thus, GAP activity is required for proper polarization and septin structure formation during chemotropic growth.

Defining the Spatial Distribution of Proteins at the Site of Polarity

A significant challenge in single-cell analysis is to relate the behavior of individual cells to general trends in the population. This is a particular challenge when tracking the localization of proteins on the leading edge of the cell, given that they display significant heterogeneity in space and over time. We reasoned that by using the polar cap as a point of reference, we would be able to discern patterns in protein distribution across the leading edge. To that end, we developed a method to conduct pairwise spatial comparisons of a given protein to active Cdc42 (indicated by Bem1-GFP). Our method is analogous to one used previously to compare the temporal activation of Rho family members in mammalian cells [34]. Specifically, we generated Cdc3 profiles at each time point, using the peak intensity of Bem1 as a common reference point. The data were then normalized such that the fluorescence distribution at each time point sums to 1, and averaged for 25 or more individual cells ([Figure 5](#), top). We further combined the data (time points >150 min) to create a single distribution for protein localization versus distance from peak Cdc42-GTP ([Figure 5](#), bottom).

As shown in [Figure 5](#), septins were properly resolved from the polar cap in wild-type cells starting at ~120 min. The separation was evident after treatment with either 0–150 nM or 300 nM pheromone, but was more pronounced in elongating cells than in shmooing cells (compare [Figures 5A and 5B](#)). Again, the observed differences in septin separation are expected, given the larger size of the leading edge in elongating cells. Cells lacking Sst2 showed a strong (aberrant) accumulation of septins at the polar cap following treatment with 300 nM pheromone (shmoo formation) but a mostly flat septin distribution at 0–150 nM pheromone (elongated morphology). The flat distribution of septins should not be interpreted as a complete lack of septin structures; rather, any septin structures were likely to be randomly distributed with respect to the polar cap, and therefore the location of the polar cap would not be predictive of septin localization. The profiles of the receptor-uncoupled *sst2^{Q304N}* and the GAP-deficient *gpa1^{G302S}* mutants resembled wild-type and *sst2Δ* cells, respectively ([Figures 5B and 5C](#)). By this approach, we consistently saw a spike of

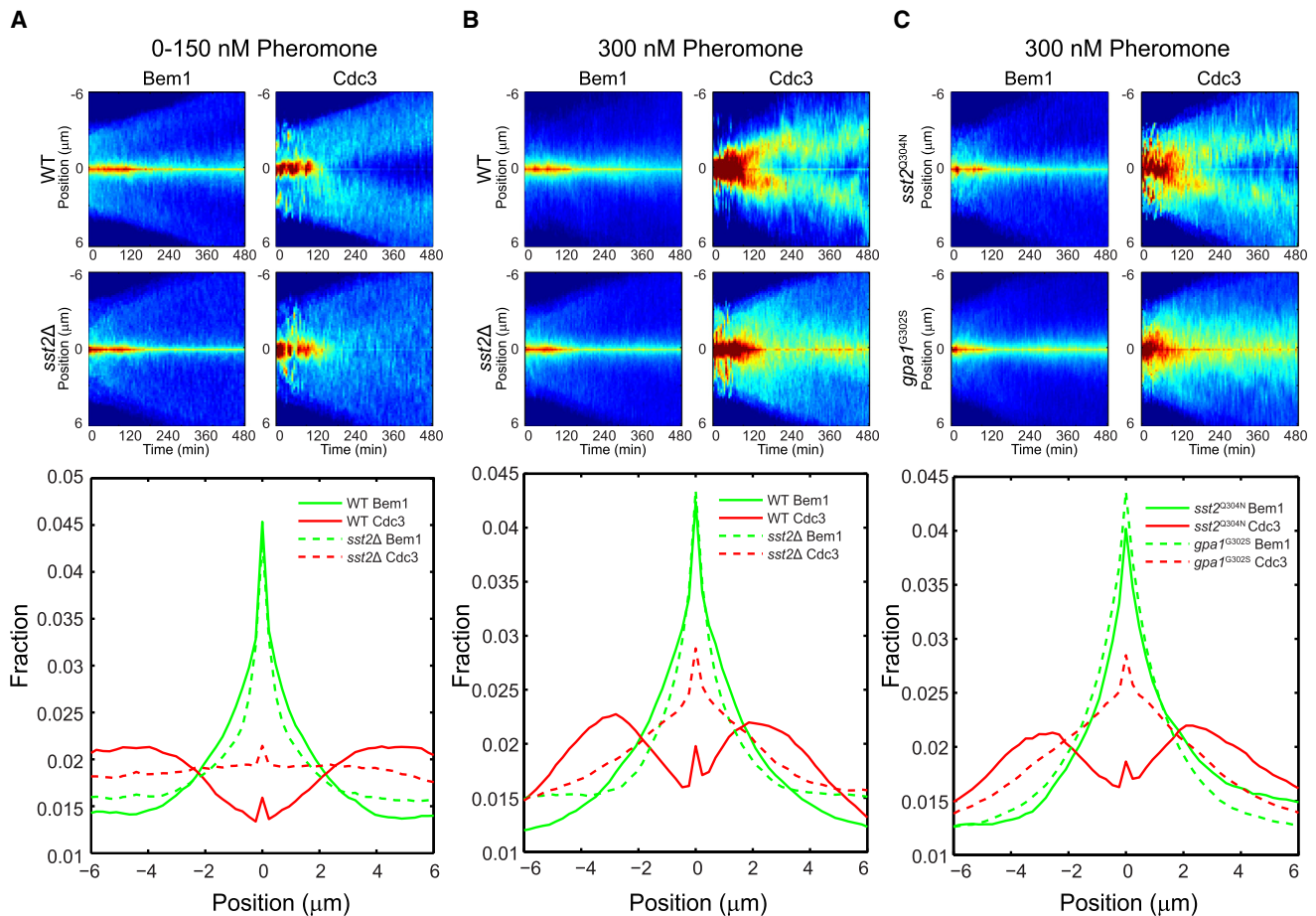


Figure 5. Determining the Profile of Proteins on the Leading Edge

(A) Average kymographs for wild-type and *sst2Δ* cells in a gradient of pheromone. Individual-cell kymographs were spatially normalized to peak Bem1 and then averaged across all cells. Data were used to calculate the spatial distribution (lower graph) of Cdc3 and Bem1, normalized to Bem1 by averaging the data in the kymographs from 150 to 480 min. Profiles sum to 1, and can be thought of as probability distributions.

(B and C) As in (A); average kymographs and spatial profiles for (B) wild-type and *sst2Δ* and (C) *sst2^{Q304N}* and *gpa1^{G302S}* cells in high pheromone. The spike in Cdc3 at peak Bem1 is not due to bleedthrough.

Data shown are derived from the experiments shown in Figures 2, 3, and 4.

Cdc3 at the peak Bem1 position, perhaps indicative of the known recruitment of septins by Gic1/2 and Cdc42-GTP [35, 36]. This new method of analysis provides quantitative information about the position of septins relative to Bem1 and, more broadly, can be used to compare the position of any membrane-associated protein relative to the polar cap. Below we use this method to compare distributions of different proteins across multiple strains.

GAP Function Promotes Focused Exocytosis

We next considered the role of Sst2 in membrane trafficking. Exocytosis and endocytosis are important for the establishment of polarity and for gradient tracking in yeast [37–40]. Exocytosis is responsible for delivery of proteins to the site of polarity, and has been implicated in polar cap wandering as well as the promotion of gradient tracking [29]. Moreover, the delivery of naive vesicles to the polar cap may help push septins into their characteristic ring shape, as occurs during budding [26]. Conversely, endocytosis removes proteins as they diffuse toward the periphery of the polar cap [38, 39].

Given the potential roles of vesicle trafficking in polarity and in septin structure formation, we next examined the role of

Sst2 GAP activity in endocytosis and exocytosis. To that end, we examined the distribution of known markers for endocytosis (Ede1-GFP) [41] and exocytosis (Exo84-GFP) [42] relative to the polar cap in both wild-type and the GAP-deficient *gpa1^{G302S}* strains treated with 300 nM pheromone (Figure 6A). The regions of exocytosis and endocytosis are diagrammed in Figure 6B, where each line represents the median distance of the marker protein from the center of the polar cap.

As shown in Figure 6C, we observed the same relative distribution of Bem1 and the endocytic marker in both the wild-type and the GAP-deficient mutant cells. Cells lacking GAP activity exhibited an unusual broadening in the distribution of the exocytic marker; however, there was no change in the shape of the marker when aligned to itself (Figure S3A). Thus, the observed distribution arose from increased variability in the site of exocytosis relative to the polar cap. Likewise, the mutant cells exhibited mislocalized septins with a broadened distribution similar to that of the endocytic marker. These data indicate that the GAP activity of Sst2 is necessary to restrict the area in which exocytosis occurs, and to promote separation of septins from sites of endocytosis.

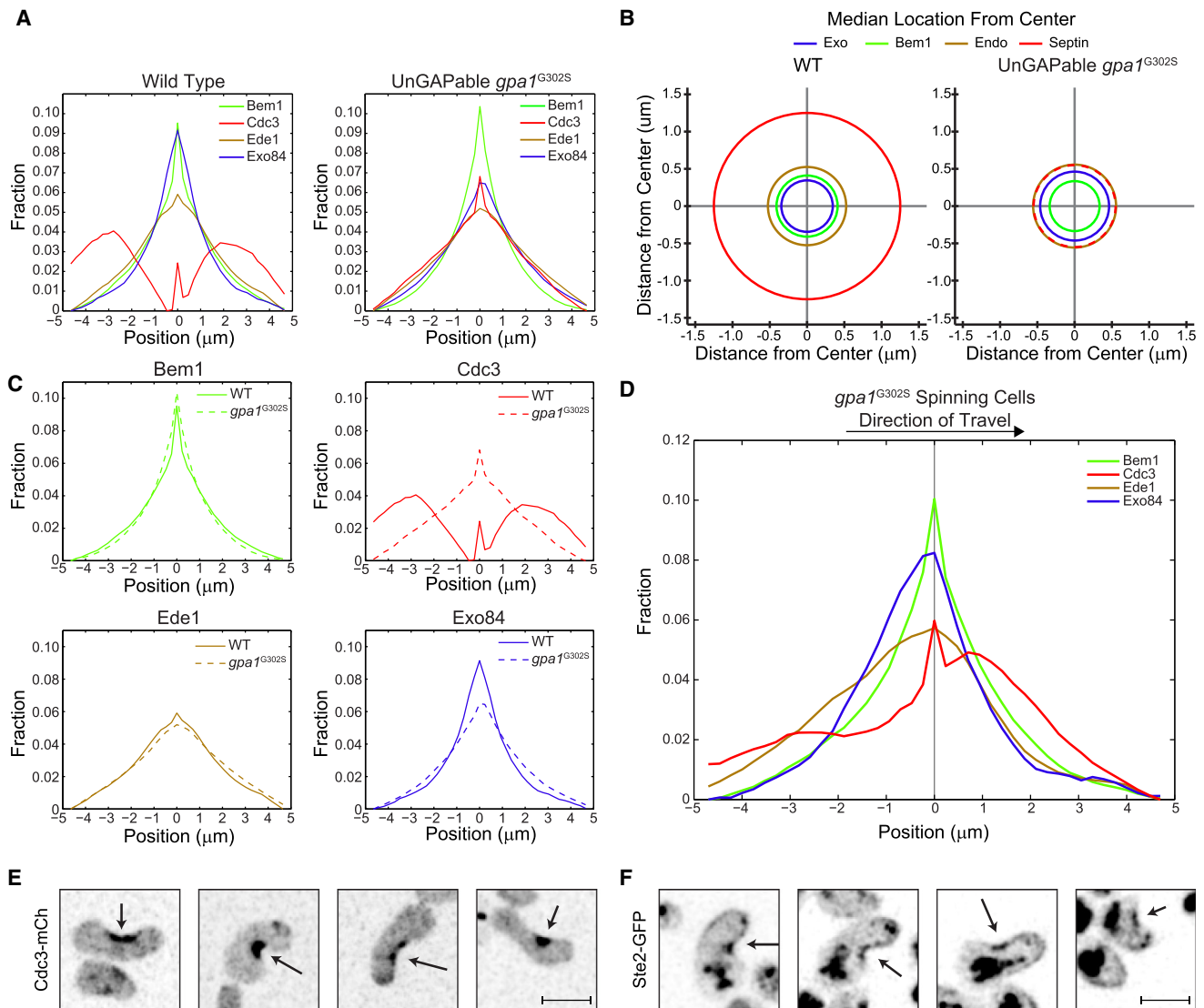


Figure 6. Sst2 Promotes Focused Exocytosis and Separation of Septins from Sites of Endocytosis

(A) The profile of an endocytic marker (Ede1-GFP) normalized spatially to Bem1-mCherry, and an exocytic marker (Exo84-GFP) normalized spatially to Bem1-mCherry in wild-type and *gpa1*^{G302S} cells (Ede1-mCherry normalized to Bem1-GFP used in the mutant strain), exposed to 300 nM uniform pheromone. Data are derived from 30 cells from two independent experiments (Exo84), 20 cells from two independent experiments (Ede1), 42 cells from two independent experiments (*gpa1*^{G302S} Exo84), and 51 cells from three independent experiments (*gpa1*^{G302S} Ede1).

(B) Representation of the median distance of each protein from the center of the polar cap for wild-type and *gpa1*^{G302S} cells.

(C) Pairwise comparisons of Bem1, Cdc3, Ede1, and Exo84 in wild-type and *gpa1*^{G302S} cells. Bem1 and Cdc3 profiles are from same data set as Figure 5.

(D) Spatial profile of Bem1, Cdc3, Ede1, and Exo84 in *gpa1*^{G302S} cells that are spinning (all data are plotted as spinning to the right). Data are representative of 1,105 time points from 17 cells from two independent experiments (Bem1 and Cdc3), 934 time points from 26 cells from two independent experiments (Ede1), and 699 time points from 17 cells from two independent experiments.

(E and F) Wild-type cells expressing Cdc3-mCherry (E) or Ste2-GFP during elongation (F) (the strong signal in the interior of the cell is GFP in the vacuole). Arrows indicate the accumulation of protein at the plasma membrane on the inside of turns. Images are representative of two independent experiments for both Cdc3 and Ste2. The scale bars represent 5 μ m.

See also Figure S3.

The defects in septin localization were most evident in cells that were spinning. This correlation prompted us to ask whether septins might influence the direction of travel. To that end, we sorted the septin profiles into two groups based on the direction of movement. When we oriented each of the profiles in the same direction and averaged the distribution, we observed a striking enrichment of septins in advance of the polar cap (Figure 6D). Whereas the polar cap moved toward septins, it moved away from the sites of exocytosis

and endocytosis. Both types of trafficking were asymmetrically distributed behind the polar cap (~67% higher frequency behind the cap than in front of the cap; Figures S3B and S3C). Based on current models [29], the asymmetric distribution of exocytosis would be predicted to drive movement of the polar cap in the opposite direction of the fusion event.

Although the trend to move toward septins was most obvious in the *gpa1*^{G302S} mutant, the same phenomenon was evident in those rare wild-type cells that were initially

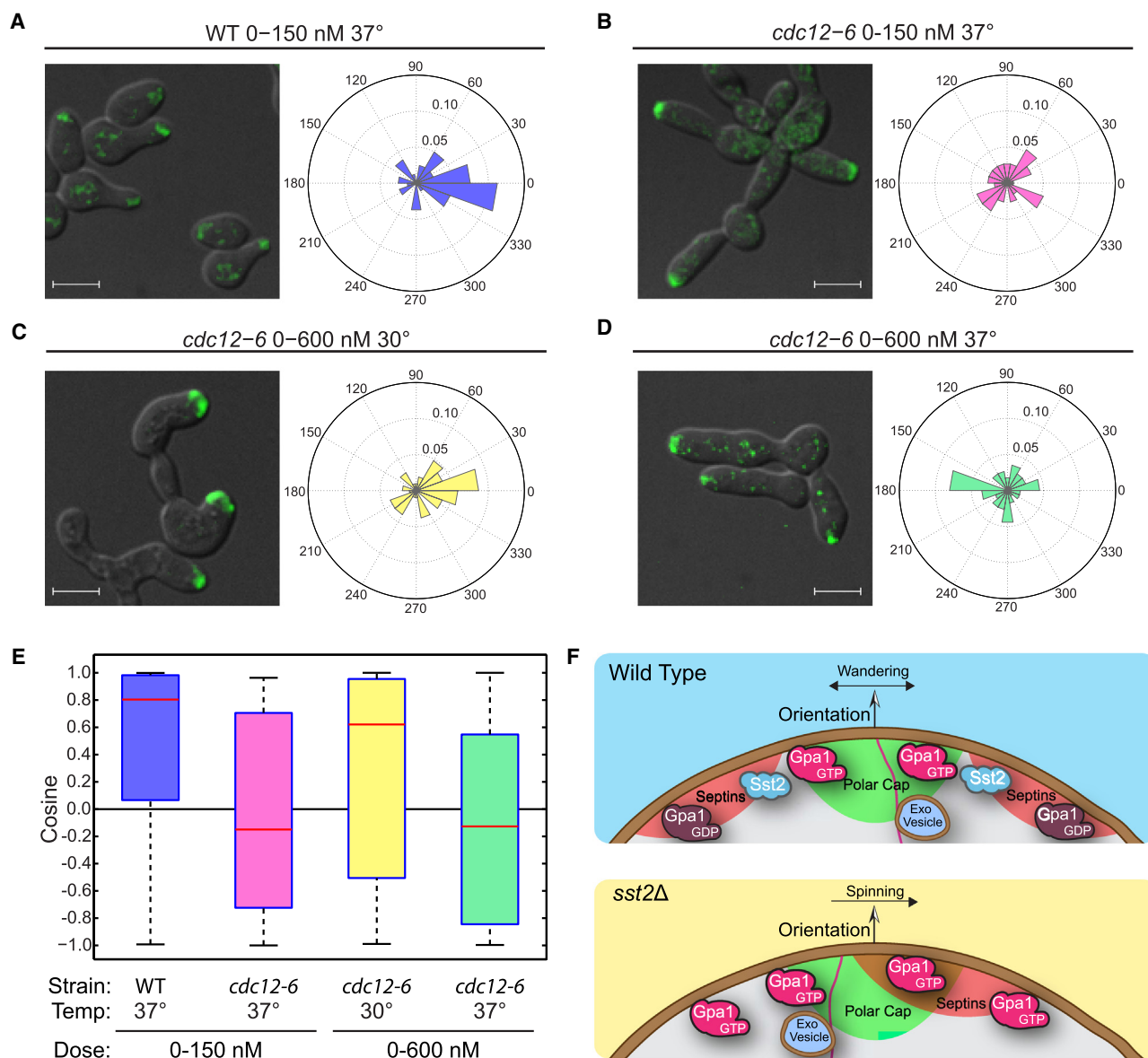


Figure 7. Septins Are Required for Gradient Tracking

(A–D) Wild-type (A) ($n = 40$) and *cdc12-6* cells (B) ($n = 56$) expressing Bem1-GFP were exposed to a 0–150 nM gradient of pheromone (high on the right) at 37°C. Gradient tracking was assessed at 3 hr and is displayed as a polar histogram. Bar length represents the fraction of cells oriented to the given angle; 0° is upgradient. The *cdc12-6* strain was also exposed to a 0–600 nM gradient at (C) 30°C ($n = 52$) and (D) 37°C ($n = 56$). The scale bars represent 5 μ m. (E) Boxplot of the cosines of the angles from (A)–(D). A cosine of 1 indicates orientation with the gradient, whereas -1 indicates orientation opposite the gradient. Strains that are not able to track a gradient will have a median cosine of 0. The box indicates the 25th to 75th percentiles; the red line is the median. All data are from two independent experiments.

(F) The role of Sst2 in gradient tracking. In wild-type cells, Sst2 is localized to the septin structures surrounding the polar cap and promotes conversion of Gpa1-GTP to Gpa1-GDP. Exocytic events occur near the center of the polar cap, driving wandering. In the absence of Sst2, septins no longer exclude the polar cap, biasing exocytic events to the opposite side of the polar cap relative to septins. The biased exocytic events push the polar cap consistently toward the septins, resulting in sharp turns, or spinning of the polar cap around the periphery of the cell.

misaligned and had to turn toward the gradient (Figure 6E). Thus, in addition to restricting the range of motion of the polar cap, it appears that septins direct the polar cap toward the pheromone stimulus. The septins, in turn, are most likely to follow the pheromone receptor Ste2. In support of this idea, we found that receptors were consistently enriched, together with septins, on the inside of turning cells (Figures 6E and 6F). From these data, we conclude that septins bias the direction of polar cap movement.

Our results indicated that septin structures bias polar cap movement in cells that are turning, as occurs during gradient tracking. Thus, we considered whether septins are needed to track a gradient. For these experiments, we tested a strain bearing a temperature-sensitive septin mutation, *cdc12-6* [43]. As shown in Figure 7, the mutant strain was unable to track a 0–150 nM gradient at the restrictive temperature. To accommodate the response at the higher temperature, we also tested the *cdc12-6* strain in a 0–600 nM gradient. The

mutant strain was able to properly track a gradient at the semi-permissive temperature (30°C) but not at the fully restrictive temperature (37°C). The septin-deficient cells still elongated in a straight line (Figures 7B and 7D), suggesting that the tracking defect was due to an inability of the cells to turn and that any septin boundary function is unnecessary for persistent polar cap movement. Taken together, our data indicate that Sst2 is required for proper septin organization, and that organized septins are required to dynamically regulate polar cap movement in response to a pheromone stimulus.

Discussion

Here we describe several new and unexpected functions for two well-known signaling proteins. In particular, we show that the RGS protein Sst2 is required for proper septin organization, and that septins are required for proper gradient tracking. By orienting cell expansion toward a weak pheromone gradient, the RGS and septins work together to promote cell-cell interactions leading to mating. In the absence of RGS function, septin structures are disorganized and become colocalized with the polar cap. As a consequence, the polar cap turns past the source of pheromone and the cell expands in the wrong direction. Thus, in the absence of well-organized septins, cells no longer track a gradient of pheromone.

Central to our analysis was the development of a new computational method for determining the spatial distribution of membrane proteins. By this method, we have shown that the polar cap is bounded by septins and by Sst2. In the absence of Sst2, the septins no longer exclude the polar cap. However, the septins may nevertheless function as a barrier to exocytic events, because exocytosis occurs asymmetrically, away from septin structures. Measuring the probability distribution of proteins at the leading edge, as we have done here, could be used to inform both deterministic and probabilistic models of cell signaling. By performing the analysis over time for single cells, such distribution profiles can be sorted based on metadata such as angle of orientation of the polar cap, direction of travel, and speed of travel. With sufficiently fast sampling, the approach could lead to improved understanding of how trafficking influences morphogenesis.

Whereas septins are well known to facilitate mitosis, their contribution to other morphogenic states has received little attention. During mitosis, septins form a characteristic double-ring structure that is thought to prevent the exchange of membrane proteins between mother and daughter cells [22]. In pheromone-treated cells, septins instead assemble as parallel fibers that would presumably allow some diffusion of the polar cap [28]. Our observations reveal additional important differences between mitotic and chemotrophic cells. Although septins are necessary for proper budding, we have shown here that they are dispensable for elongated cell growth. Another major difference between mitosis and chemotrophic growth is the role of Sst2. Although Sst2 is not required for mitosis, we have shown here that it is required for proper septin organization during chemotrophic growth. In mitotic cells, septins recruit the GAPs for Cdc42 [44, 45]. It has recently been suggested by Okada et al. that the association of Cdc42 GAPs with the septin ring forms a negative feedback loop necessary for septin ring formation during mitosis [26]. In chemotrophic cells, septins do not recruit GAPs for Cdc42 (Figure S4) but instead recruit Sst2, the GAP for Gpa1. Thus, whereas mitotic cells exhibit localized inactivation of Cdc42, chemotrophic cells limit the activation of Cdc42 indirectly

through inhibition of Gpa1. In either case, the polar cap is destabilized in the vicinity of the septin ring, leading to directed cellular expansion.

Although septins are dispensable for forming elongated structures, they are required for turning toward a gradient. This indicates that the septin barrier function is dispensable for persistent growth. Rather, it is likely that the mislocalization of septins, seen in *sst2Δ* cells, leads to aberrant turning and inability to track a gradient. This observation is consistent with earlier findings that mislocalized septins can lead to morphological defects [46].

Another contributor to cell polarization is vesicle trafficking. There is emerging evidence that exocytosis of vesicles clears existing proteins from the site of delivery, thereby pushing the septins into their characteristic ring structure [26]. Because the exocytic vesicles lack activated Cdc42, these fusion events are likely to trigger some degree of wandering by the emerging polar cap [29]. Conversely, it is unclear whether endocytosis has the ability to influence polar cap movement. Rather, endocytosis is thought to promote the removal of proteins as they diffuse away from the leading edge, thereby restricting their distribution to an area surrounding the polar cap [38, 39].

Taken together, our findings reveal a likely mechanism by which RGS proteins and septins cooperate to promote gradient tracking behavior (Figure 7). During chemotrophic growth, as in mitosis, septins set the boundary for polar cap migration and the delivery of exocytic vesicles. In contrast to mitosis, these septin structures assemble over a much larger area, are more diffuse, and are more dynamic. Because of its relatively broad distribution in chemotrophic cells, the polar cap has more opportunity to wander [29, 40]. Such wandering behavior would presumably allow the cell to change polar cap orientation and improve gradient tracking [29]. When Sst2 is absent, the septins are malformed and polar cap wandering is exaggerated. The loss of Sst2 does not affect mitosis because the mitotic septin ring structure fixes the polar cap position, and the site of bud emergence does not change over time or in the presence of an external stimulus [25].

In conclusion, we have defined a new role for RGS proteins as regulators of septin organization, distinct from their role as regulators of G protein signaling. Further, we have defined a new role for septins in chemotrophic growth, distinct from their role in mitotic cell division. Given the similarities in G protein signaling across species, our findings are likely to find parallels in more complex systems, including neutrophil migration and cancer metastasis.

Experimental Procedures

All experiments were performed in a BY4741 background. Cells were maintained in and grown in 2% dextrose yeast peptone (YPD) or synthetic complete (SCD) medium with appropriate selection. Yeast strains were made through standard methods. Imaging of cells was performed in SCD filtered in a 0.22 μm 1 l filter system (Corning). Microfluidic experiments were performed as described previously [21], using an Olympus Revolution XD (Olympus/Andor) spinning disk confocal microscope. Image analysis was performed using Fiji (Fiji Is Just ImageJ; <http://fiji.sc/Fiji>) [47] and MATLAB (MathWorks). MATLAB scripts are available upon request. For detailed methods, see [Supplemental Experimental Procedures](#).

Supplemental Information

Supplemental Information includes Supplemental Experimental Procedures, four figures, two tables, and six movies and can be found with this article online at <http://dx.doi.org/10.1016/j.cub.2014.11.047>.

Author Contributions

J.B.K., T.C.E., and H.G.D. conceived the study, designed the experiments, and wrote the manuscript. J.B.K. performed the microscopy experiments, constructed strains, and designed and performed image analysis. G.D. constructed strains and performed the microscopy experiments. J.B.S. performed image analysis. S.P.V. performed the Ste2 experiments.

Acknowledgments

We would like to thank Jeff Hasty for the microfluidics mold and Danny Lew for the gift of reagents and helpful discussions. We would also like to thank Beverly Errede, Denis Tsygankov, and Maria Minakova for helpful discussions. This work was supported by NIH grants GM080739 (to H.G.D.) and GM103870 and GM079271 (to T.C.E.) and by American Heart Association postdoctoral fellowship 11POST7600017 (to J.B.K.).

Received: August 12, 2014

Revised: October 26, 2014

Accepted: November 17, 2014

Published: January 15, 2015

References

- Kolaczowska, E., and Kubes, P. (2013). Neutrophil recruitment and function in health and inflammation. *Nat. Rev. Immunol.* 13, 159–175.
- Arkowitz, R.A. (2009). Chemical gradients and chemotropism in yeast. *Cold Spring Harb. Perspect. Biol.* 1, a001958.
- Segall, J.E. (1993). Polarization of yeast cells in spatial gradients of α mating factor. *Proc. Natl. Acad. Sci. USA* 90, 8332–8336.
- Wang, Y., and Dohlman, H.G. (2004). Pheromone signaling mechanisms in yeast: a prototypical sex machine. *Science* 306, 1508–1509.
- Dohlman, H.G., and Thorner, J.W. (2001). Regulation of G protein-initiated signal transduction in yeast: paradigms and principles. *Annu. Rev. Biochem.* 70, 703–754.
- Park, H.O., and Bi, E. (2007). Central roles of small GTPases in the development of cell polarity in yeast and beyond. *Microbiol. Mol. Biol. Rev.* 71, 48–96.
- Butty, A.C., Pryciak, P.M., Huang, L.S., Herskowitz, I., and Peter, M. (1998). The role of Far1p in linking the heterotrimeric G protein to polarity establishment proteins during yeast mating. *Science* 282, 1511–1516.
- Nern, A., and Arkowitz, R.A. (1999). A Cdc24p-Far1p-G $\beta\gamma$ protein complex required for yeast orientation during mating. *J. Cell Biol.* 144, 1187–1202.
- Bi, E., and Park, H.O. (2012). Cell polarization and cytokinesis in budding yeast. *Genetics* 191, 347–387.
- Slaughter, B.D., Smith, S.E., and Li, R. (2009). Symmetry breaking in the life cycle of the budding yeast. *Cold Spring Harb. Perspect. Biol.* 1, a003384.
- Casamayor, A., and Snyder, M. (2002). Bud-site selection and cell polarity in budding yeast. *Curr. Opin. Microbiol.* 5, 179–186.
- Moore, T.I., Tanaka, H., Kim, H.J., Jeon, N.L., and Yi, T.M. (2013). Yeast G-proteins mediate directional sensing and polarization behaviors in response to changes in pheromone gradient direction. *Mol. Biol. Cell* 24, 521–534.
- Shimada, Y., Gulli, M.P., and Peter, M. (2000). Nuclear sequestration of the exchange factor Cdc24 by Far1 regulates cell polarity during yeast mating. *Nat. Cell Biol.* 2, 117–124.
- Erdman, S., and Snyder, M. (2001). A filamentous growth response mediated by the yeast mating pathway. *Genetics* 159, 919–928.
- Valtz, N., Peter, M., and Herskowitz, I. (1995). FAR1 is required for oriented polarization of yeast cells in response to mating pheromones. *J. Cell Biol.* 131, 863–873.
- Hao, N., Nayak, S., Behar, M., Shanks, R.H., Nagiec, M.J., Errede, B., Hasty, J., Elston, T.C., and Dohlman, H.G. (2008). Regulation of cell signaling dynamics by the protein kinase-scaffold Ste5. *Mol. Cell* 30, 649–656.
- Elion, E.A., Satterberg, B., and Kranz, J.E. (1993). FUS3 phosphorylates multiple components of the mating signal transduction cascade: evidence for STE12 and FAR1. *Mol. Biol. Cell* 4, 495–510.
- Dohlman, H.G., and Thorner, J. (1997). RGS proteins and signaling by heterotrimeric G proteins. *J. Biol. Chem.* 272, 3871–3874.
- Apanovitch, D.M., Slep, K.C., Sigler, P.B., and Dohlman, H.G. (1998). Sst2 is a GTPase-activating protein for Gpa1: purification and characterization of a cognate RGS-G α protein pair in yeast. *Biochemistry* 37, 4815–4822.
- Ballon, D.R., Flanary, P.L., Gladue, D.P., Konopka, J.B., Dohlman, H.G., and Thorner, J. (2006). DEP-domain-mediated regulation of GPCR signaling responses. *Cell* 126, 1079–1093.
- Dixit, G., Kelley, J.B., Houser, J.R., Elston, T.C., and Dohlman, H.G. (2014). Cellular noise suppression by the regulator of G protein signaling Sst2. *Mol. Cell* 55, 85–96.
- Gladfelter, A.S., Pringle, J.R., and Lew, D.J. (2001). The septin cortex at the yeast mother-bud neck. *Curr. Opin. Microbiol.* 4, 681–689.
- Caudron, F., and Barral, Y. (2009). Septins and the lateral compartmentalization of eukaryotic membranes. *Dev. Cell* 16, 493–506.
- Takizawa, P.A., DeRisi, J.L., Wilhelm, J.E., and Vale, R.D. (2000). Plasma membrane compartmentalization in yeast by messenger RNA transport and a septin diffusion barrier. *Science* 290, 341–344.
- Barral, Y., Mermall, V., Mooseker, M.S., and Snyder, M. (2000). Compartmentalization of the cell cortex by septins is required for maintenance of cell polarity in yeast. *Mol. Cell* 5, 841–851.
- Okada, S., Leda, M., Hanna, J., Savage, N.S., Bi, E., and Goryachev, A.B. (2013). Daughter cell identity emerges from the interplay of Cdc42, septins, and exocytosis. *Dev. Cell* 26, 148–161.
- Giot, L., and Konopka, J.B. (1997). Functional analysis of the interaction between Afr1p and the Cdc12p septin, two proteins involved in pheromone-induced morphogenesis. *Mol. Biol. Cell* 8, 987–998.
- Longtine, M.S., Fares, H., and Pringle, J.R. (1998). Role of the yeast Gin4p protein kinase in septin assembly and the relationship between septin assembly and septin function. *J. Cell Biol.* 143, 719–736.
- Dyer, J.M., Savage, N.S., Jin, M., Zyla, T.R., Elston, T.C., and Lew, D.J. (2013). Tracking shallow chemical gradients by actin-driven wandering of the polarization site. *Curr. Biol.* 23, 32–41.
- Butty, A.C., Perrinjaquet, N., Petit, A., Jaquenoud, M., Segall, J.E., Hofmann, K., Zwahlen, C., and Peter, M. (2002). A positive feedback loop stabilizes the guanine-nucleotide exchange factor Cdc24 at sites of polarization. *EMBO J.* 21, 1565–1576.
- Gulli, M.P., Jaquenoud, M., Shimada, Y., Niederhäuser, G., Wiget, P., and Peter, M. (2000). Phosphorylation of the Cdc42 exchange factor Cdc24 by the PAK-like kinase Cla4 may regulate polarized growth in yeast. *Mol. Cell* 6, 1155–1167.
- Tong, Z., Gao, X.D., Howell, A.S., Bose, I., Lew, D.J., and Bi, E. (2007). Adjacent positioning of cellular structures enabled by a Cdc42 GTPase-activating protein-mediated zone of inhibition. *J. Cell Biol.* 179, 1375–1384.
- DiBello, P.R., Garrison, T.R., Apanovitch, D.M., Hoffman, G., Shuey, D.J., Mason, K., Cockett, M.I., and Dohlman, H.G. (1998). Selective uncoupling of RGS action by a single point mutation in the G protein α -subunit. *J. Biol. Chem.* 273, 5780–5784.
- Machacek, M., Hodgson, L., Welch, C., Elliott, H., Pertz, O., Nalbant, P., Abell, A., Johnson, G.L., Hahn, K.M., and Danuser, G. (2009). Coordination of Rho GTPase activities during cell protrusion. *Nature* 461, 99–103.
- Iwase, M., Luo, J., Nagaraj, S., Longtine, M., Kim, H.B., Haarer, B.K., Caruso, C., Tong, Z., Pringle, J.R., and Bi, E. (2006). Role of a Cdc42p effector pathway in recruitment of the yeast septins to the presumptive bud site. *Mol. Biol. Cell* 17, 1110–1125.
- Sadian, Y., Gatsogiannis, C., Patasi, C., Hofnagel, O., Goody, R.S., Farkasovský, M., and Raunser, S. (2013). The role of Cdc42 and Gic1 in the regulation of septin filament formation and dissociation. *eLife* 2, e01085.
- Brennwald, P., and Rossi, G. (2007). Spatial regulation of exocytosis and cell polarity: yeast as a model for animal cells. *FEBS Lett.* 581, 2119–2124.
- Valdez-Taubas, J., and Pelham, H.R. (2003). Slow diffusion of proteins in the yeast plasma membrane allows polarity to be maintained by endocytic cycling. *Curr. Biol.* 13, 1636–1640.
- Marco, E., Wedlich-Soldner, R., Li, R., Altschuler, S.J., and Wu, L.F. (2007). Endocytosis optimizes the dynamic localization of membrane proteins that regulate cortical polarity. *Cell* 129, 411–422.
- Layton, A.T., Savage, N.S., Howell, A.S., Carroll, S.Y., Drubin, D.G., and Lew, D.J. (2011). Modeling vesicle traffic reveals unexpected consequences for Cdc42p-mediated polarity establishment. *Curr. Biol.* 21, 184–194.
- Gagny, B., Wiederkehr, A., Dumoulin, P., Winsor, B., Riezman, H., and Hagenauer-Tsapis, R. (2000). A novel EH domain protein of

- Saccharomyces cerevisiae*, Ede1p, involved in endocytosis. *J. Cell Sci.* 113, 3309–3319.
42. Guo, W., Grant, A., and Novick, P. (1999). Exo84p is an exocyst protein essential for secretion. *J. Biol. Chem.* 274, 23558–23564.
 43. Adams, A.E., and Pringle, J.R. (1984). Relationship of actin and tubulin distribution to bud growth in wild-type and morphogenetic-mutant *Saccharomyces cerevisiae*. *J. Cell Biol.* 98, 934–945.
 44. Smith, G.R., Givan, S.A., Cullen, P., and Sprague, G.F., Jr. (2002). GTPase-activating proteins for Cdc42. *Eukaryot. Cell* 1, 469–480.
 45. Caviston, J.P., Longtine, M., Pringle, J.R., and Bi, E. (2003). The role of Cdc42p GTPase-activating proteins in assembly of the septin ring in yeast. *Mol. Biol. Cell* 14, 4051–4066.
 46. Gladfelter, A.S., Kozubowski, L., Zyla, T.R., and Lew, D.J. (2005). Interplay between septin organization, cell cycle and cell shape in yeast. *J. Cell Sci.* 118, 1617–1628.
 47. Schindelin, J., Arganda-Carreras, I., Frise, E., Kaynig, V., Longair, M., Pietzsch, T., Preibisch, S., Rueden, C., Saalfeld, S., Schmid, B., et al. (2012). Fiji: an open-source platform for biological-image analysis. *Nat. Methods* 9, 676–682.